Supplemental Materials

Degradation of perfluorooctane sulfonate via *in-situ* electro-generated ferrate and permanganate oxidants in NOM-rich source waters

Sean T. McBeath, Nigel J.D. Graham

Table S1. Ultrahigh-performance liquid chromatography mobile phase flow gradient conditions.

Time, *min*	**Flow,** mL min^{-1}	**%A**[a]	**%B**[b]
0.00		70.0	30.0
3.00		0.00	100.0
5.00	0.500	0.00	100.0
5.10		70.0	30.0
6.00		70.0	30.0

[a] *Ammonium acetate buffer (2 mM)*
[b] *Methanol*

Table S2. Mass spectrometry PFOS analysis conditions.

Source	Capillary (kV)	0.44
	Sampling Cone	60
	Source Offset	80
Temperature	Source (ºC)	150
	Desolvation (ºC)	650
Gas Flow	Cone Gas (L h^{-1})	30
	Desolvation Gas (L h^{-1})	1200
	Nebuliser (bar)	6.5

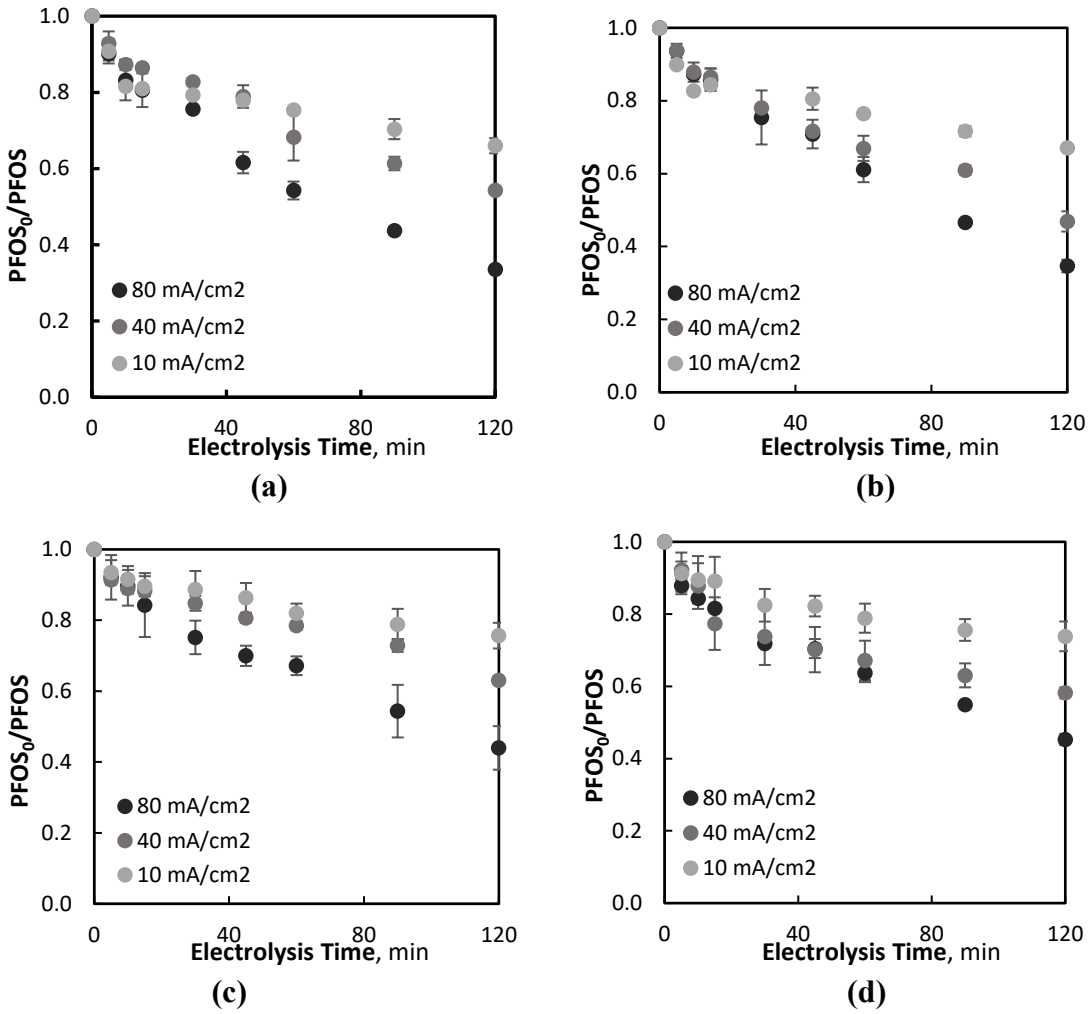

Fig. S1. PFOS degradation during simultaneous EO and ferrate oxidation, at 10, 40 and 80 mA cm^{-2} conditions, and at an initial iron (Fe^{2+}) concentration of: (a) 179 µM, (b) 54 µM, (c) 18 µM, and (d) 9 µM.

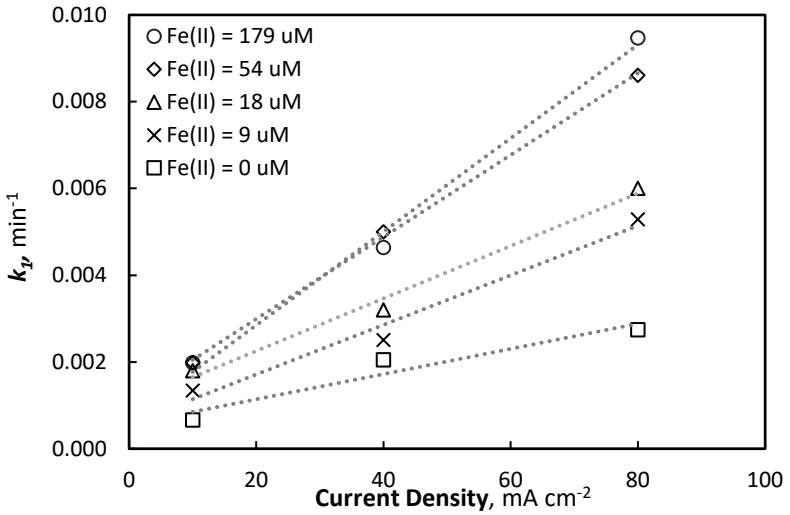

Fig. S2. Pseudo-first-order rate constants of PFOS degradation at various current densities and initial Fe^{2+} concentrations.

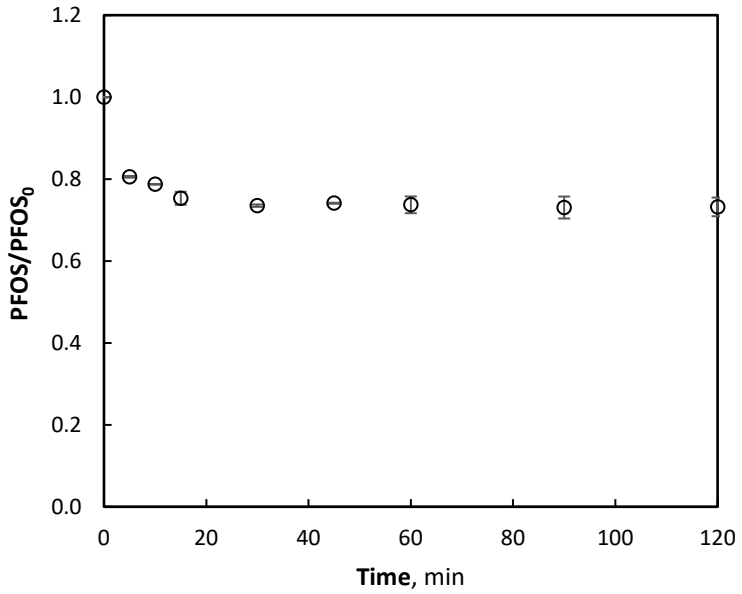

Fig. S3. Electrochemically synthesised ferrate oxidation of PFOS ($PFOS_0$ = 400 μg L^{-1}, $Fe(VI)_0$ = 17.3 μM, pH = 7, T = 21.0 ± 0.8°C).

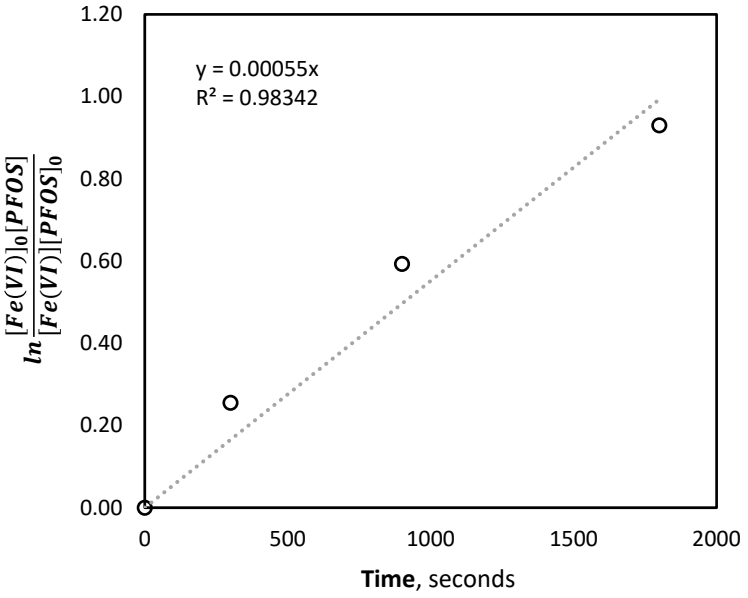

Figure S4. Second-order reaction linear plot for PFOS degradation via electrochemically synthesized ferrate over 30 minutes ($PFOS_0$ = 400 µg L^{-1}, $Fe(VI)_0$ = 17.3 µM, pH = 7, T = 21.0 ± 0.8°C).

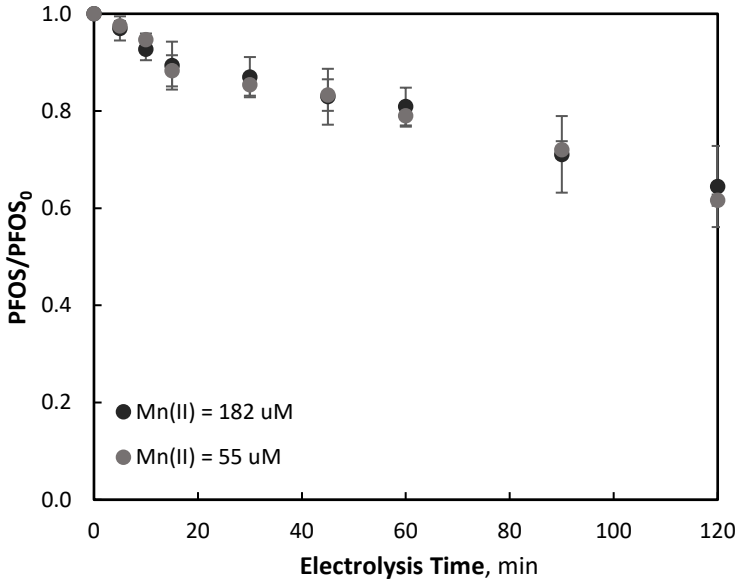

Figure S5. Simultaneous EO and permanganate oxidation of PFOS during 80 mA cm^{-2} electrolysis ($PFOS_0$ = 400 µg L^{-1}, pH = 7, T = 21.0 ± 0.8°C).

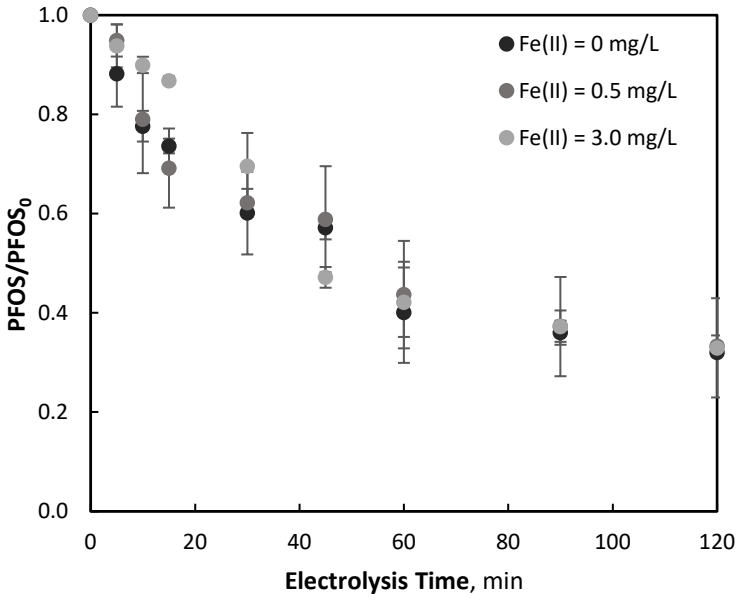

Fig. S6. PFOS degradation at 80 mA cm^{-2} in NOM-containing water (DOC_0 = 2.956 mg L^{-1}, UV_{254} = 0.098 cm^{-1}, $PFOS_0$ = 400 µg L^{-1}, pH = 7, T = 21.0 ± 0.8°C).

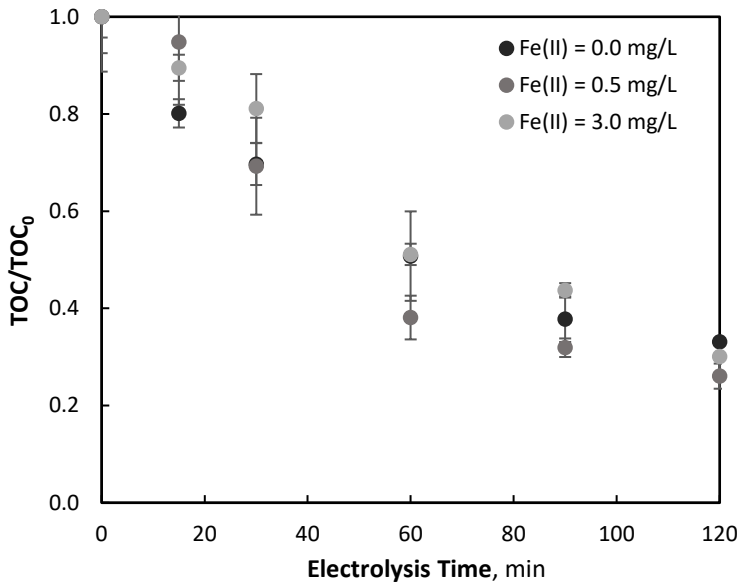

Figure S7. DOC reduction at 80 mA cm^{-2} in NOM-containing water (DOC_0 = 2.956 mg L^{-1}, UV_{254} = 0.098 cm^{-1}, $PFOS_0$ = 400 µg L^{-1}, pH = 7, T = 21.0 ± 0.8°C).

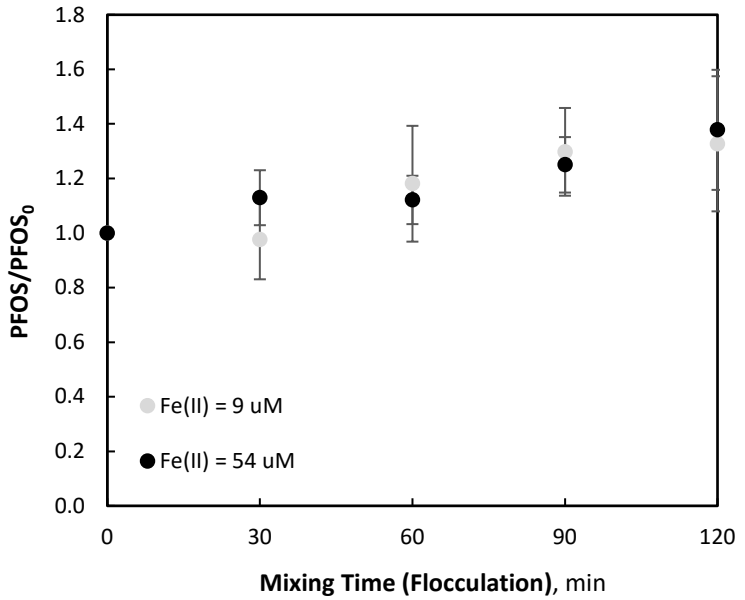

Figure S8. PFOS concentration during coagulation/flocculation tests, after EO.

S.1 PFOS oxidation by-product identification method

PFOS oxidation by-products were identified using the UPLC-MS/MS (Waters Synapt G2-Si high definition mass spectrometry), in the MS analysis mode. No collision energy or fragments were considered, but all other conditions (column, column temperature, injection volume, mobile phase composition and flow rate, etc.) remained the same as that previously described for PFOS quantification (*Section 3.2.2*) and Table S1.

S.2 Oxidation by-product formation

No clear PFOS degradation pathway could be determined or confidently proposed based on the oxidation by-products identified throughout electrolysis for both EO and simultaneous EO and ferrate oxidation, as well as ferrate only oxidation. While the concentrations of by-products were not pursued in detail, as an objective of this study, the prevalence and appearance of key species were identified. The predominant species identified throughout all PFOS degradation experiments included: pentafluoroethane sulfonic acid, perfluoroheptane sulfonic acid (PFHpS), trifluoroacetic acid (TFA), perfluoropentane sulfonic acid (PFPeS), perfluorohexane sulfonic acid (PFHxS), pentafluorobutanesulfonic acid (PFBS) and pentafluoropropionic acid (PFPrA), as well as several other species that were identified in trace amounts.

During the EO process and simultaneous EO-ferrate process, an initial sharp increase of PFHpS was observed for the first 10 minutes of electrolysis, followed by a steady decline for the remainder of the electrolysis time. PFHpS is structurally similar to PFOS, with a seven-carbon chain, and provided the highest MS response (chromatogram peak area). This suggests the carbon furthest from the sulfonate group is the most susceptible to direct electrochemical oxidation and may be the primary site of PFOS degradation. Other predominant sulfonate species that were identified included PFHxS (6-carbon chain), PFPeS (5-carbon chain), PFBS (4-carbon chain) and pentafluoroethane sulfonate (2-carbon chain), which all yielded increased peak areas throughout the 120 minutes of electrolysis. Also detected throughout electrolysis was TFA, which may account for some of the fluorocarbon species which were removed from PFOS and the other aforementioned sulfonate by-products. The only difference in by-product formation observed during

the EO process and the simultaneous EO-ferrate process was the formation of PFPrA in the former, which may the due of competition for direct oxidation sites when aqueous iron is present in the water matrix (during simultaneous EO-ferrate oxidation). In addition to these by-products, a MS low response indicating low concentrations of PFOA, perfluoropropanesulfonic acid, perfluorocaleric acid and 4-deoxypentonic acid, was detected. A summary of the oxidation by-product species observed is shown in Figure S9.

During ferrate oxidation experiments, fewer oxidation by-products were observed, which would be expected as PFOS degradation was comparatively limited when compared to the EO process. Three sulfonate-containing by-products, namely PFHpS (7-carbon chain), PFHxS (6-carbon chain) and pentafluoroethane sulfonate (2-carbon chain), were observed to increase over the 120 minutes of contact time. Similarly, TFA was once again observed throughout the reaction with a low MS response, once again potentially accounting for some of the fluorocarbon molecules which are removed from PFOS and the other sulfonate-containing by-products.

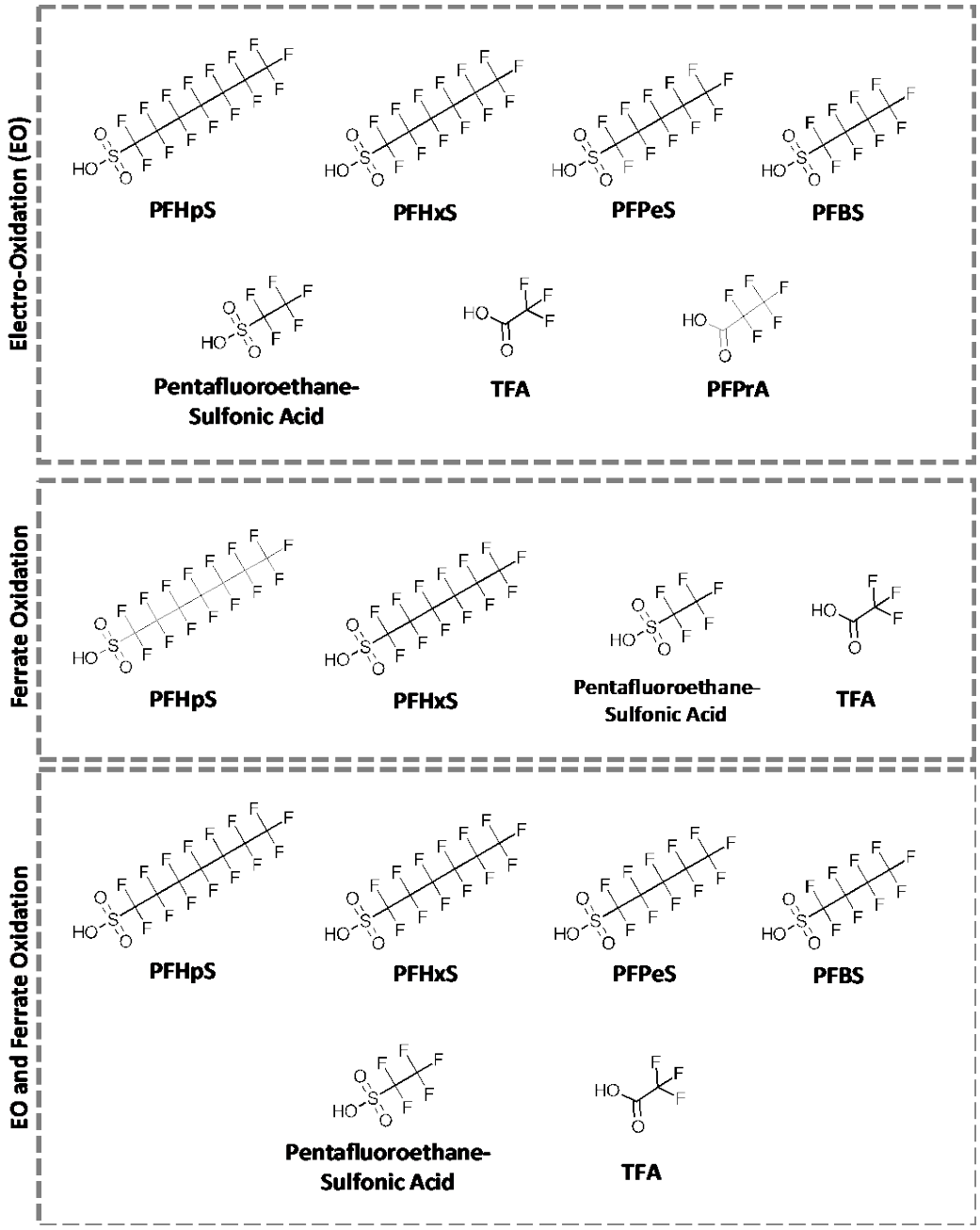

125

126 **Fig. S9.** Identified PFOS oxidation by-products during EO, ferrate oxidation, and simultaneous EO and

127 ferrate oxidation.

128

129

130